Submitted to Physics in Medicine and Biology

UCRL-19487
Preprint

c.3

NEUTRON RADIOGRAPHY AND DOSIMETRY IN HUMANS: THEORETICAL STUDIES

Thomas F. Budinger, Robert J. Howerton,
and Ernest F. Plechaty

April 1970

RECEIVED
LAWRENCE
RADIATION LABORATOR
MAY 27 1970
LIBRARY AND
DOCUMENTS SECTI

AEC Contract No. W-7405-eng-48

TWO-WEEK LOAN COPY

This is a Library Circulating Copy which may be borrowed for two weeks. For a personal retention copy, call Tech. Info. Division, Ext. 5545

LRL

UCRL-19487

LAWRENCE RADIATION LABORATORY
UNIVERSITY of CALIFORNIA BERKELEY

DISCLAIMER

This document was prepared as an account of work sponsored by the United States Government. While this document is believed to contain correct information, neither the United States Government nor any agency thereof, nor the Regents of the University of California, nor any of their employees, makes any warranty, express or implied, or assumes any legal responsibility for the accuracy, completeness, or usefulness of any information, apparatus, product, or process disclosed, or represents that its use would not infringe privately owned rights. Reference herein to any specific commercial product, process, or service by its trade name, trademark, manufacturer, or otherwise, does not necessarily constitute or imply its endorsement, recommendation, or favoring by the United States Government or any agency thereof, or the Regents of the University of California. The views and opinions of authors expressed herein do not necessarily state or reflect those of the United States Government or any agency thereof or the Regents of the University of California.

UCRL-19987
4/70

Neutron Radiography and Dosimetry in Humans: Theoretical Studies

THOMAS F. BUDINGER, B.S., M.S.,M.D.,
Lawrence Radiation Laboratory, Berkeley, California
and
ROBERT J. HOWERTON, B.S.,M.S.,
ERNEST F. PLECHATY, B.S.,
Lawrence Radiation Laboratory, Livermore, California

1. Introduction

Although conventional roentgenography usually provides adequate contrast for imaging living biological systems, there are some situations such as the delineation of soft tissue tumour masses and non-bony tissue abnormalities for which conventional techniques are inadequate. During the last decade investigations have been carried out to determine whether neutron radiography might complement or supplant x-ray radiography for certain clinical and research applications (Gerrard 1968 and Berger 1965). Since neutrons and x-ray energy photons interact with matter through quite different mechanisms, it was hoped that these differences would manifest themselves as useful radiological techniques. For neutron kinetic energies greater than 10 ev, neutrons interact only with atomic nuclei while photons of energies less than several Mev interact primarily with the entire atomic or molecular system. (For energies less than about 10 ev, neutrons also interact with bound molecules.

As early as 1956, Thewlis (1956) at AERE, Harwell, successfully imaged plant tissues by use of thermal neutrons as the incident particles. Subsequently,

Berger (1962) showed excellent contrast in a thermal neutron radiograph of the grasshopper. More recently Atkins (1965) at Brookhaven National Laboratory, Barton (1964) at Harwell, England, and Brown and Parks (1969) at Savannah River Laboratory obtained radiographs of thin ($\leq$3 cm) biological samples. These successful experiments with thin samples were generally accomplished by shining a beam of thermal neutrons through the sample such that the transmitted beam impinged upon a dysprosium or indium loaded plate. Dysprosium and indium have exceptionally high probability for capture of thermal neutrons, thus leading to radioactive residual nuclei. The activated plate was then "developed" by bringing it into intimate contact with an x-ray film in a conventional autoradiography mode.

As the thickness of the biological samples is increased, the results become progressively poorer because the dominant thermal neutron-nucleus interaction is elastic, which causes diffusion of the incident neutrons. An analogous situation would be an attempt to photograph an object embedded in frosted glass.

In an attempt to extend the thickness of biological materials for which useful thermal neutron radiographs could be made, several clever techniques were investigated. The results with thermal and epithermal neutrons can be summed up as disappointing. Antiscatter grids led to better images than had previously been obtained for 3 cm thick biological material, but the quality was much poorer than that obtained by x-ray radiography (Atkins 1965). Fast neutron radiography has received some attention experimentally and theoretically. The first human radiographs were published in 1964 by Anderson and co-workers (Anderson, Osborn, and Tomlinson 1964) at Harwell, England, but were of poor resolution.

In order to understand the potentials of practical neutron radiography of living human parts, we performed numerical experiments to simulate neutron radiography of thick tissue with idealized neutron detection. The calculations reported here were made with a Monte Carlo neutronics code on a CDC-6600. The purpose was to examine the degree of contrast of bone and muscle for a better understanding of the feasibility of this mode of imaging and, secondly, to calculate in some

detail the dose deposited at various locations in the tissue, detail the dose deposited at various locations in the tissue, including muscle, bone, bone marrow, and surface skin. Previous calculations did not use realistic geometrics or differentiate the dose between these dissimilar biological materials.

2. Methods

2.1. General

The simulated upper arm was 24 cm in length and 6 by 10 cm elliptical in cross section. The neutrons were assumed to impinge uniformly on an area 10 cm by 2 cm perpendicular to the 10 cm arm dimension (fig. 1). A centrally oriented cylindrical bone simulating a humerus had a diameter of 4 cm and cortex thickness of 0.75 cm. Thus the marrow cavity was 2.5 cm in diameter. The atom composition for all significant elements was used to describe soft tissue, bone, and marrow (table 1).

Numerical experiments were conducted by exposing the 2 cm wide strip to 100 000 neutrons of 1 kev, 120 kev, fission spectrum, and 14 Mev. Both single and multiple neutron scattering inside and outside the 2 cm wide strip were treated explicitly by the

calculational method. With the exception of neutron upscattering in the thermal region, all physical phenomena are accounted for by the calculational method. For all incident neutron energies except thermal, the lack of treatment of thermal upscattering is of no consequence. It is felt that even for thermal neutrons this is only a second-order perturbation.

The energy deposited was tallied for 20 zones within the 2 by 10 cm band. Trajectories of neutrons transmitted through or leaking from the system were stored and planar plots of these neutrons obtained for various distances from the arm, thus simulating an ideal plane detector or imaging device. These details are discussed below.

2.2. Atomic composition of the human upper arm

The atomic composition of an arm was simulated from the known composition of muscle, fat, and bone as detailed in table 1. The values for lean muscle shown in table 1 are a synthesis of published values in various handbooks. The values for muscle were derived from an over-all figure of 18.5% protein, which figure includes the controversial 3% bicarbonate. Values of 6% lipid and 2% glycogen were

used. The water content was 76%. The major additional elements are based on values reported by Widdowson and Dickerson (1964). The density of muscle is 1 gm/cc.

Satisfactory values for bone composition are somewhat more difficult to obtain. For cortical bone the best value for the ash content is 63% by weight (Gong, Arnold, and Cohn 1964a). The water content varies with the type of bone and age, but for adult cortical bone is 12%. The organic composition, which is primarily protein and little if any fat, is 25%. Of the 63% ash, almost 100% is hydroxyapatite with only small contributions from sodium, chlorine, and magnesium. The values for calcium and phosphorus are based on the assumption that 99% is hydroxapatite. The abundance of hydrogen in fat is similar to that in muscle and, for all practical purposes, the mean free paths of neutrons in these two tissues are identical. The density of bone is 2 gm/cc for the moist living state (Gong, Arnold, and Cohn 1964b).

The atomic composition of muscle and marrow as used for this study does not differ significantly from the atomic composition of the standard man used for

the calculations reported in Handbook 63 (National Bureau of Standards Handbook, 1967). However, the bone composition differs significantly for every element. In particular, the hydrogen atom percentage is one-half that of muscle; nitrogen is three times more abundant; and calcium and phosphorus are present in quantities of 7.8 and 4.7% respectively, whereas in muscle only insignificant quantities of these mineral elements are present.

2.3. Neutron transport and energy deposit calculations

Any neutronics calculations, to be satisfactory, require both a good calculational method and a good set of input constants. The latter describe the probability of neutron-nucleus interaction for all possible neutron induced reactions appropriate to the isotopes present in the material for which the calculation is made. The method used for these calculations is the well known Monte Carlo technique (Kimlinger and Plechaty 1968). This technique was chosen because, of all neutronics methods, it allows the least number of approximations to the physical problem being calculated. In essence, individual neutrons are followed through the material being investigated, in this case an upper arm. Statistics are kept on all neutron-

nucleus interactions until the neutron being followed disappears or leaks out of the system. At each point of neutron-nucleus interaction some energy is transferred from the neutron to another particle or is converted to radiative energy in the form of one or more (usually more) photons. This then provides the information required to calculate the energy deposited in the material. The neutron tracking procedure is repeated with a sufficient number of source neutrons to obtain statistical significance. For example, consider one neutron somewhere in the system. This neutron will have a location, a speed, and a direction. A random number is selected which, by proper application of an appropriate total cross section, will determine its next location of interaction. Because calculations involving movement from one material zone to another are more complicated, assume the next interaction location is within the same material. Another random number is chosen to determine which reaction took place. To illustrate how a random number determines the reaction type, assume there are two possible reactions with reaction cross sections in the ratio of one to three. Assign to the first reaction random numbers from zero to 0.25 and to the

second reaction random numbers from 0.25 to 1.0. Now select a random number between zero and unity. Clearly it is just three times more probable that the random number chosen will correspond to the second reaction. Having found which reaction took place, that reaction is investigated to see whether one or more neutrons result from the reaction or whether the neutron disappears. Consider the first case, which is more interesting. The direction of the outgoing neutron (assume only one) is then determined by another random number selection and application to the angular distribution appropriate to the reaction. The energy and consequently the speed of the second neutron may be determined by nuclear reaction kinematics in some cases, but in others still another random number must be chosen and properly applied. The reaction rate in each material is tallied and saved for calculation of the energy deposit, which is made after the neutron tracing is finished.

In general, the energy deposited in the form of recoil nucleus energy will be absorbed locally; that is, near where the neutron-nucleus reaction took place. The same is true for charged particle products

of the reaction. It is not true, however, that the photon energy can be assumed to be absorbed locally. The calculations done here tallied the total energy deposited and, therefore, provide an upper limit to the locally absorbed energy. That is, in these calculations photons are assumed to be absorbed locally, which is contrary to fact to some degree. More precise calculations can be made at the expense of several-fold more effort. A Monte Carlo photon-transport (Kimlinger, Plechaty, and Terrall 1967) calculation could be linked to the output of the neutron transport calculation (Kimlinger and Plechaty 1968), but for two reasons this was not done. First, the photon production data required, primarily photon energy distributions, are not well enough known for the neutron induced reactions considered here to allow meaningful calculations. The data currently available depend largely on systematics, interpolations, extrapolation, and educated guessing (Howerton and Plechaty 1968 and Yost 1967). Second, in view of the state of the data it was felt that the upper limit of energy absorbed is a more desirable value considering the conservative approach which should be adopted toward irradiating living human tissue with neutrons.

2.4. Neutron cross section data

The data used in the neutronics calculations which are largely neutron cross sections, angular distributions, energy distributions, and energy deposits are based on the Lawrence Radiation Laboratory, Livermore, evaluated neutron cross section library (Howerton, Perkins, and Doyas--to be published). For some 70 isotopes and elements and for energetically possible reactions, appropriate cross sections and related data are tabulated for neutron energies over nine decades of energy from 2.5×10^{-2} ev to 14.6×10^{6} ev, as continuous functions of energy. The tools of production of evaluated cross sections are generally experimental data, theoretical calculations, and systematics. A computerized library of experimental data (Howerton, Cahill, Hill, Thompson, and Perkins 1969) is maintained for this purpose. The library of experimental data currently contains 750 000 experimentally determined values, including essentially all the data presented in the various editions of the well known BNL-325 (Goldberg, Mughabghab, Purohit, Magurno, and May 1966) plus much which has been measured since the publication of those volumes. These

data have been accumulated with the active cooperation of the National Neutron Cross Section Center at Brookhaven National Laboratory; the Center for Collection of Neutron Constants operated at Saclay, France, by the European Nuclear Energy Agency; and the Nuclear Data Unit of the International Atomic Energy Agency at Vienna, who routinely supply Lawrence Radiation Laboratory, Livermore, with all the data they are entering into their own systems.

Most neutron cross sections are not well known. Despite the large number of measurements, most reactions have not been measured and reliable theoretical models do not exist for many reactions and all important energy ranges. This means that the cross sections for most reactions have to be estimated from systematics. Fortunately, for most calculations, the cross sections obtained from consideration of systematics give reasonable answers when used in calculations which can be compared with integral experiments. This is largely because most calculations deal with neutrons having a distribution over a wide range of energies, and the regions in which cross sections are overestimated in magnitude are balanced by those in which they are underestimated. It is especially true that

neutrons will be widely distributed in energy for any neutronically thick hydrogenous material such as the biological systems considered here. It is just for this reason that any calculations must take into account the energy dependence of the cross sections, angular distributions, and energy distributions of secondary neutrons. For example, with hydrogen, the simplest of nuclei, the elastic scattering cross section for neutron energy of 0.025 ev varies from about 22 to 80 barns, depending upon how the hydrogen is bound, while at 14 Mev the value is 0.67 barn. Likewise, the neutron capture cross section of hydrogen is about 0.35 barn at .025 ev and 0.00004 barn at 14 Mev. As the neutron energy is increased, more and more reactions become possible. For the isotopes used in the calculations described here, table 2 presents the reactions having thresholds (Howerton, Broff, Cahill, and Chazan 1964) less than 14.0 Mev, together with the half-life and disintegration mode of the reaction product.

3. Results

The best visual results from use of a simulated plane detector which recorded the position of arrival of each neutron leaking from the arm were noted for

the experiment with 120 kev neutrons incident. These results are shown for a detector 0.2 and 3 meters from the arm in fig. 2. There is a slight increase in dot density over the projected region of bone. The ratio of neutrons arriving at the projected bone region to those at the soft tissue region was 3 for 120 kev incident and not significantly different from 1 in the other experiments. As about 100 000 neutrons were followed in each experiment, the statistics are good. The number of neutrons arriving at a hypothetical film placed at 0.15 and 5 meters are plotted to simulate a densitometer trace across the results from 1 kev, 120 kev, fission spectrum, and 14 Mev experiments (fig. 3). The stippled area indicates the region of bone, and the intensity is the relative number of neutrons at 0.1 cm radial intervals for the projected arm. The opaqueness of soft tissue relative to bone is seen best at 120 kev, which is probably an optimal energy because multiple scattering is minimized, but the elastic collision cross section for hydrogen is still high relative to that of other elements and other reactions. In fact, above 4 Mev bone is more opaque than soft tissue.

Arm dosimetry calculations for the four incident energies are shown in fig. 4. The near skin doses are higher than deeper soft tissue doses and the marrow dose is slightly greater than what would be expected if there were no intervening bone. The bone dose is higher than that absorbed by contiguous soft tissues. This is primarily a result of the twofold increase in density and, for the higher energies, an increase in the number of reactions with Ca and P. The average dose absorbed for each experiment is shown in table 3. The increased bone dose applies to energy absorbed by bone matrix, protein, and hydroxyapatite. Thus in estimating marrow, soft tissue filled haversian canals, and interstitial region doses, the marrow values and not the bone dose should be used.

4. Discussion

4.1 Contrast and resolution

Scattering effects in hydrogenous material impose a limit on the material thickness which can be successfully neutron radiographed. The reported high contrast resolution of 0.1 mm in material is obtainable only for neutronically thin biological materials. Based on the loss of resolution due to multiple scattering at low energies and a similarity

of elemental cross sections at the higher energies, it should not be expected that neutron radiographs through thick tissues in the living man would be useful. Our calculations confirm these expectations. Scattered neutrons which proceed in a somewhat random direction convey little useful information about the internal structure of an object. This effect is emphasized in a material which is largely hydrogenous. Although only about 10% of the body by weight is hydrogen, there are more atoms of hydrogen than any other element in the body. The total macroscopic neutron absorption and scattering cross section for hydrogen is several orders of magnitude greater than that of the next most abundant element, oxygen. The important contrasting mechanism between muscle and bone lies in the fact that there is one-fourth the amount of hydrogen in bone compared with that in muscle.

The radiolucency of bone and the lack of attenuation by air spaces would be reflected in a neutron radiograph of a man's 20 cm thick chest (Anderson et al. 1964); however, the resolution of such a picture (Parks, Brown, and Harmer 1969) leaves neutron radiography as a very poor supplement to conventional medical x-rays. Although a two- to threefold contrast

between bone and soft tissue can be effected without any special filtering, the presence of multiple scattering seriously restricts neutron radiography as a potential tool for a diagnosis of soft tissue tumours or bony defects in humans.

4.2. Fast neutrons

The nuclear interaction characteristics of fast neutrons differ markedly from those of thermal neutrons. There has been a growing interest during the past few years in investigating the possibilities of fast neutron radiography. Sources of fast neutrons have become more readily available both as distributed energy sources such as spontaneously fissionable isotopes, e.g., ^{252}Cf (Barton 1969), and monoenergetic sources from charged particle interactions such as the 14 Mev neutrons from the D-T reaction.

The problem of successful radiography with neutrons of any energy has two inseparable facets. Not only must an acceptable image be formed, but the energy deposited within the biological tissue must be acceptably low. There is a myriad of problems associated with the detection of fast neutrons which cannot be solved by reliance on the neutron capture reaction as was done with the dysprosium or indium

loaded plates for thermal neutrons. In general, the cross section for the capture of neutrons decreases rapidly with increasing neutron energy and for neutrons in the Mev energy range will not have sufficient magnitude to be useful for the purposes described here.

The hypothesized neutron detector used for these calculations was assumed to have a flat energy response and to be planar. No such detector exists. There are, however, materials which could be investigated for use as planar detectors of neutrons for energies greater than the threshold of the reaction on which the detector is based. Many nuclides have n,2n reactions leading to radioactive residual nuclei. The thresholds of these n,2n reactions are generally in the neighborhood of 7 to 9 Mev, and the reaction cross section at 14 Mev is of the order of 1 to 2 barns. For biological materials of the order of thickness of one mean-free path (14 Mev neutrons) about 35% of the incident neutrons would be unattenuated and available for reaction in a planar surface loaded with the detector material. If the activation

cross section is high enough, the plate might be sufficiently activated to be subject to successful autoradiograph.

For example, the n,2n reaction on both naturally occurring isotopes of europium lead to radioactive residual nuclei. The thresholds of these reactions are 8.1 and 8.7 Mev for ^{151}Eu and ^{153}Eu so they might be used to detect uncollided transmitted neutrons from a 14 Mev source. Similarly, there are materials which have n,n'γ reactions leading to isomeric states of convenient half-life which might be used to detect fission spectrum neutrons above the threshold of the reaction. These matters remain to be investigated.

4.3. Validity of calculations

Estimates of neutron transport or energy deposit based on the attenuation coefficients appropriate to incident neutron energy are absolutely invalid for systems which are neutronically thicker than a small fraction ($\sim$0.1) of one mean-free path. This is especially true for a system containing light elements, notably hydrogen. On the average a single elastic collision of a neutron with a hydrogen nucleus results in a decrease of neutron energy by one-half with the other half deposited locally by the recoil

proton. Although the average energy of the scattered neutron after a collision with a proton is one-half the incident neutron energy, the scattered neutron can have any energy from zero to the incident value. An attenuation calculation can give an uncollided flux value, but for neutronically thick systems this figure is of little use and is of no use for determining dose or energy deposited in the system.

There are numerous calculational techniques which deal with the problem of neutron transport through materials of any type. Because of the complexity of the problem these techniques are reduced to practicality by means of sophisticated computer codes. As the size and calculational speed of computers have increased, the restrictions required by limited memory size and cycle time have been relaxed with the result that the neutronics calculations have become progressively more dependable. The neutronics codes which have the closest simulation to physical reality are those using the Monte Carlo method. With sophisticated Monte Carlo neutronics codes, using good values of neutron cross sections, calculated neutron transport and energy deposit values when compared with experiment have been shown to be reliable to

accuracies ranging from a few percent to a few tenths of a percent for physical configurations similar to the problems considered here.

4.4. Neutron fluence

The average dose received by the arm, based on the results of the Monte Carlo calculations, is shown in table 3. This dose was calculated by summing the energy deposited in each of 20 energy deposition zones and normalising for the fluence and the mass of the irradiated volume. The dose deposited by 14 Mev neutrons incident is 100 times greater than the dose deposited by 1 kev incident neutrons. However, there is an equally large difference in the number of neutrons transmitted; e.g., in the case of 1 kev only one in every 350 neutrons is detected under poor geometry conditions, or one in 2000 for good geometry. Whereas, in the case of 14 Mev neutrons, one neutron is detected for every two neutrons incident for both the good and poor geometry situations. Thus, if the energy deposited is normalized for a number of transmitted neutrons, the energy deposited by 14 Mev neutrons will be less than that by 1 kev; but, the types of reactions differ markedly in the two cases, and the resolution of any picture

from 1 kev will be necessarily much poorer and perhaps of little value because of multiple scattering. Another way of evaluating the dose vs. resolution situation is to note that for equivalent density of detected neutrons, those from 1 kev incident have suffered multiple scattering, and thus information loss is greater than for 14 Mev neutrons. However, there is no marked difference in bone and tissue cross sections at 4 Mev (table 4); thus, the 4 Mev particle will be scattered equally by bone and soft tissue. At 14 Mev bone is relatively opaque compared with soft tissue, because the mean-free path is relatively less in bone at higher energies.

The results of these calculations are in close accordance with other calculations and measurements of the National Bureau of Standards (1967), Smith and Boot (1962), and Humphreys and Sayeg (1968). Computer neutron radiography simulation on thin objects is being explored by Porter and Robinson (1969). The major contribution of our studies is the simulation of a realistic geometry including bone. The slightly increased marrow dose compared with contiguous soft tissue is what one would expect for epithermal neutrons which are moderated by intervening tissue.

The almost twofold increase of dose deposited to bone cortex by neutrons has not been noted by others, probably because all the reactions of above-thermal-energy neutrons in bone have not been included in their calculations.

Considering the increase in knowledge regarding cross sections and the importance of understanding distributed dose between bone, bone marrow, and soft tissue, we hope to extend these studies to other parts of the human body, not for neutron radiography feasibility studies, but for radiation protection dose calculations and neutron cancer therapy applications.

5. Conclusions

Neutron radiography for delineating soft-tissue tumours or bone lesions results in an unsatisfactory image contrast for tissues thicker than approximately 3 cm according to Monte Carlo calculations using 1 kev, 120 kev, fission spectrum, and 14 Mev neutrons incident on a 6 cm thick arm. There was, at most, a threefold increase in contrast between bone and soft tissue for 120 kev incident neutrons. These theoretical studies corroborate neutron radiographs of small mammals taken by others. There are some very

specialized situations for which a neutron radiograph might helpfully supplement a routine roentgenograph.

Of more immediate and practical significance, this study shows the difference in dose deposited to tissue, bone cortex, and marrow for a realistic geometry of a simulated human arm. The neutron dose to bone is approximately twice that to contiguous soft tissue.

This research was supported in part by the Cancer Research Coordinating Committee of the University of California, and the U. S. Atomic Energy Commission. We appreciate the helpful suggestions of Dr. Hans Bichsel, Dr. Patricia Durbin-Heavey, and Mr. H. Wade Patterson.

ABSTRACT

Calculations using Lawrence Radiation Laboratory, Livermore, SORS Monte Carlo computer code and neutron cross section library were done on a simulated human arm, including bone and marrow, for 1 kev, 120 kev, fission spectrum, and 14 Mev incident monoenergetic neutrons. These studies were done to analyse the dose distributed to bone and marrow, and to determine the feasibility of neutron radiography as a practical clinical tool. The resolution possible through tissues thicker than approximately 3 cm makes neutron radiography impractical except for possibly very special circumstances. The dose calculations reveal as much as a twofold increase in dose deposited in the bone cortex compared with surrounding contiguous tissues. The skin dose is approximately two times greater than the dose 3 cm inside the tissue. The average energy absorbed in the arm on the basis of a fluence of one neutron incident per cm^2 is 0.5×10^{-10} rad, 1.6×10^{-10} rad, 10×10^{-10} rad, 40.4×10^{-10} rad, for 1 kev, 120 kev, fission spectrum, and 14 Mev neutrons, respectively.

References

Anderson, J., Osborn, S. B., and Tomlinson, R. W. S., 1964, Neutron radiation in man. Brit. J. Radiol., 37, 957.

Atkins, H. L., 1965, Biological application of neutron radiography. Materials Evaluation, 453.

Barton, J. P., 1964, Some possibilities of neutron radiography. Phys. Med. Biol., 9, 33.

_____, 1969, Neutron radiography, in Californium-252 progress no. 1. USAEC report, pp. 20 and 21, Savannah River Operations Office, South Carolina, October.

Berger, H., 1962, Neutron radiography. Scientific American, 207, 107.

_____, 1965, Neutron radiography: methods, capabilities, and applications (New York: Elsevier Publishing Co.).

Brown, M., and Parks, P. B., 1969, Neutron radiography in biologic media. Am. J. Roentgenol., 106, 472.

Brown, M., Allen, J. J., and Parks, P. B., 1969, Slow neutron imaging of fatty tissue through deuteration with heavy water, in Biomedical Sciences Instrumentation, Vol. 6: Proceedings of the Seventh Annual Biomedical Sciences Instrumentation Symposium on Imagery in Medicine,

May 19-22, 1969, Ann Arbor, pp. 98-103 (Pittsburgh: Instrument Society of America).

Gerrard, M., 1968, Uses of neutron radiography. Oak Ridge National Laboratory report ORNL-IIC-16, October, pp. 1-20.

Goldberg, M. D., Mughabghab, S. F., Purohit, S. N., Magurno, B. A., and May, V. M., 1966, Neutron cross sections. Brookhaven National Laboratory report BNL-325, 2nd. Ed. and supplements.

Gong, J. K., Arnold, J. S., and Cohn, S. H., 1964, Composition of travecular and cortical bone. Anat. Rec., 149, 325.

_____, 1964, The density of organic and volatile and non-volatile inorganic components of bone. Anat. Rec., 149, 319.

Howerton, R. J., Braff, D., Cahill, W. J., and Chazan, N., 1964, Thresholds of neutron induced reactions. Lawrence Radiation Laboratory report UCRL-14000, May, pp. 1-37.

Howerton, R. J., and Plechaty, E. F., 1968, A formalism for calculation of neutron induced gamma ray production, cross sections and spectra. Nucl. Sci. Eng., 32, 173.

Howerton, R. J., Cahill, W. J., Hill, K. L., Thompson, D. W., and Perkins, S. T., 1969, System for production of neutronics and photonics constants, ECSIL (Experimental Cross Section Information Library). Lawrence Radiation Laboratory report UCRL-50400, Vol. 1, Rev. 1, February, pp. 1-103.

Howerton, R. J., Perkins, S. T., and Doyas, R. J. (to be published). Lawrence Radiation Laboratory report UCRL-50400, Vol. 4. This volume will present the background and formats of the evaluated cross section library; the magnetic tape containing the data is available from the Lawrence Radiation Laboratory, Livermore, California.

Humphreys, K. C., and Sayeg, J. A., 1968, Nuclear accident dosimetry, depth-dose calculations. USAEC report EGG-1183-2165, October, p. 23, EG&G, Santa Barbara Division.

Kimlinger, J. R., Plechaty, E. F., and Terrall, J. R., 1967, SORS Monte Carlo photon transport code for the CDC-6600. Lawrence Radiation Laboratory report UCRL-50358, December, pp. 1-42.

Kimlinger, J. R., and Plechaty, E. F., 1968, SORS Monte Carlo neutron transport code for the CDC-6600. Lawrence Radiation Laboratory report UCRL-50532, October, pp. 1-29.

National Bureau of Standards Handbook 63, 1967, Protection against neutron radiation up to 30

million electron volts. NBS Handbook 63, April, pp. 40-62, U. S. Government Printing Office, Washington, D. C.

Parks, P. B., Brown, M., and Harmer, D. S., 1969, Problems of fast neutron radiography, in Biomedical Sciences Instrumentation, Vol. 6: Proceedings of the Seventh Annual Biomedical Sciences Instrumentation Symposium on Imagery in Medicine, May 19-22, 1969, Ann Arbor, pp. 118-126 (Pittsburgh: Instrument Society of America).

Porter, C. R., and Robinson, A. H., ibid., pp. 109-117.

Smith, J. W., and Boot, S. J., 1962, The variation of neutron dose with depth in a tissue-equivalent phantom. Phys. Med. Biol., 7, 45.

Thewlis, J., 1956, Neutron radiography. Brit. J. App. Phys., 7, 345.

Widdowson, E. M., and Dickerson, J. W. T., 1964, Chemical composition of the body, in Mineral metabolism, the elements, Vol. 2, Pt. A, pp. 4-207 (New York: Academic Press).

Yost, K. J., 1967, A formalism for the calculation of neutron capture gamma-ray spectra. Oak Ridge National Laboratory report ORNL-TM-1867, June, pp. 1-25.

Table 1. Atomic composition of muscle, bone, and marrow

	Muscle		Bone		Marrow	
Element	Fraction by weight	Atom %	Fraction by weight	Atom %	Fraction by weight	Atom %
^{1}H	0.107	63.9	0.030	37.35	0.116	63.7
^{16}O	0.726	27.1	0.423	32.90	0.301	10.3
^{12}C	0.153	7.6	0.125	12.97	0.558	25.5
^{14}N	0.030	1.2	0.04	3.56	0.012	0.4
^{23}Na	0.0008	0.02	0.004	0.22		
^{24}Mg	0.0004	0.01	0.004	0.21		
^{31}P	0.0001	0.001	0.116	4.66		
^{35}Cl	0.0008	0.01	0.002	0.07		
^{40}Ca	0.0001	0.001	0.252	7.84		
^{32}S	0.002	0.04	0.005	0.19		

Table 2. Significant neutron interactions

Material	Reaction	Threshold (Mev)	Half-life	Disintegration mode
$^{1}_{1}H$	Elastic scattering	0	∞	--
	n,γ	0	∞	--
$^{12}_{6}C$	Elastic scattering	0	∞	--
	n,n'γ	4.8	∞	--
	n,p	13.6	0.01 sec	β^+, 3α
	n,α	6.2	∞	--
	n,n'3α	8.0	∞	--
$^{14}_{7}N$	Elastic scattering	0	∞	--
	n,n'γ	4.0	∞	--
	n,γ	0	∞	--
	n,2n	11.3	9.96 min	β^+, γ
	n,p	0	5730 yr	β^-
	n,d	5.7	∞	--
	n,t	4.3	∞	--
	n,α	0.16	∞	--
	n,n'p	8.1	∞	--
	n,n'd	11.0	∞	--
	n,n'α	12.4	∞	--
$^{16}_{8}O$	Elastic scattering	0	∞	--
	n,n'γ	6.1	∞	--
	n,γ	0	∞	--
	n,p	10.2	7.14 sec	β^-, γ
	n,d	10.5	∞	--
	n,α	2.4	∞	--
	n,n'α	7.6	∞	--
$^{23}_{11}Na$	Elastic scattering	0	∞	--
	n,n'γ	0.45	∞	--
	n,γ	0	15 h	β^-, γ
	n,2n	13.0	2.6 yr	β^+, γ
	n,p	3.8	38 sec	β^-, γ
	n,d	6.8	∞	--
	n,t	11.2	∞	--
	n,α	4.0	11.5 sec	β^-, γ
	n,n'p	9.2	∞	--
	n,n'α	11.0	∞	--

(continued)

Table 2 (contd.)

Material	Reaction	Threshold (Mev)	Half-life	Disintegration mode
$^{24}_{12}Mg$	Elastic scattering	0	∞	--
	n,γ	0	∞	--
	n,n'γ	1.4	∞	--
	n,p	4.9	15 h	β^-, γ
	n,d	9.8	∞	--
	n,^{3}He	13.3	∞	--
	n,α	2.7	∞	--
	n,n'p	12.2	∞	--
	n,n'α	9.7	∞	--
$^{25}_{12}Mg$	Elastic scattering	0	∞	--
	n,γ	0	∞	--
	n,n'γ	0.6	∞	--
	n,2n	7.6	∞	--
	n,p	3.1	60 sec	β^-, γ
	n,d	10.2	15 h	β^-, γ
	n,t	10.9	∞	--
	n,α	0	∞	--
	n,n'p	12.6	15 h	β^-, γ
	n,n'α	10.3	∞	--
$^{26}_{12}Mg$	Elastic scattering	0	∞	--
	n,γ	0	9.5 min	β^-, γ
	n,n'γ	1.85	∞	--
	n,2n	11.6	∞	--
	n,p	8.1	1 sec	β^-, γ
	n,d	12.4	1 min	β^-, γ
	n,α	5.7	38 sec	β^-, γ
	n,n'α	11.0	∞	--
$^{31}_{15}P$	Elastic scattering	0	∞	--
	n,γ	0	14.3 days	β^-
	n,n'γ	0.6	∞	--
	n,2n	12.7	2.5 min	β^-, γ
	n,p	0.7	2.6 h	β^-, γ
	n,d	5.2	∞	--
	n,t	9.7	∞	--
	n,^{3}He	13.5	6.6 min	β^-, γ
	n,α	2.0	2.3 min	β^-, γ
	n,n'p	7.5	∞	--
	n,n'α	10.0	∞	--

(continued)

Table 2 (contd.)

Material	Reaction	Threshold (Mev)	Half-life	Disintegration mode
$^{35}_{17}Cl$	Elastic scattering	0	∞	--
	n,γ	0	3×10^5 yr	β^-
	n,n'γ	1.2	∞	--
	n,2n	13.0	32 min	β^+, γ
	n,p	0	88 days	β^-
	n,d	4.3	∞	--
	n,t	9.6	∞	--
	n,^{3}He	9.8	24 days	β^-
	n,α	0	14.3 days	β^-
	n,n'p	7.5	∞	--
	n,n'α	10.0	∞	--
$^{37}_{17}Cl$	Elastic scattering	0	∞	--
	n,γ	0	37.3 min	β^-, γ
	n,n'γ	0.84	∞	--
	n,2n	10.6	3×10^5 yr	β^-
	n,p	4.1	5.1 min	β^-, γ
	n,d	6.3	∞	--
	n,t	10.1	88 days	β^-
	n,α	1.3	12.4 sec	β^-, γ
	n,n'p	8.6	∞	--
	n,n'α	8.1	24.4 days	β^-
$^{40}_{20}Ca$	Elastic scattering	0	∞	--
	n,γ	0	8×10^4 yr	E.C.
	n,n'γ	3.5	∞	--
	n,p	0.55	∞	--
	n,d	6.3	∞	--
	n,t	13.2	7.7 min	β^+, γ
	n,^{3}He	7.2	∞	--
	n,α	0	35 days	E.C.
	n,n'p	8.6	∞	--
	n,n'α	7.2	∞	--

Table 3. Whole arm dose

Energy	Dose ($rad/n/cm^2 \times 10^9$)
1 kev	0.05
120 kev	0.16
Fission	1.0
14 Mev	4.0

Table 4. Mean free paths for selected energies

Energy (Mev)	Muscle (cm)	Bone (cm)
2×10^{-8}	0.53	0.77
2×10^{-6}	0.54	0.80
2×10^{-5}	0.54	0.80
2×10^{-4}	0.54	0.80
2×10^{-3}	0.54	0.81
2×10^{-2}	0.62	0.92
2×10^{-1}	1.04	1.40
2.0	3.46	3.94
4.1	4.32	4.24
10.1	8.29	7.52
14.1	9.08	7.59

FIGURE LEGENDS

Fig. 1. Experimental configuration for numerical simulation of neutrons impinging on an arm.

Fig. 2. Simulated neutron radiograph (upper) compared with conventional x-ray of human upper arm. Neutron quantity through central region (bone) is 3 times greater than through surrounding tissue (muscle).

Fig. 3. Comparison of contrast obtainable by using various energies of incident neutrons. Curves simulate densitometer plot from the central marrow region to the skin surface. Significant contrast is seen only for 120 kev experiment on the detector 3 meters from the arm.

Fig. 4. Energy deposited vs. arm depth for various exposures through different arm sections.

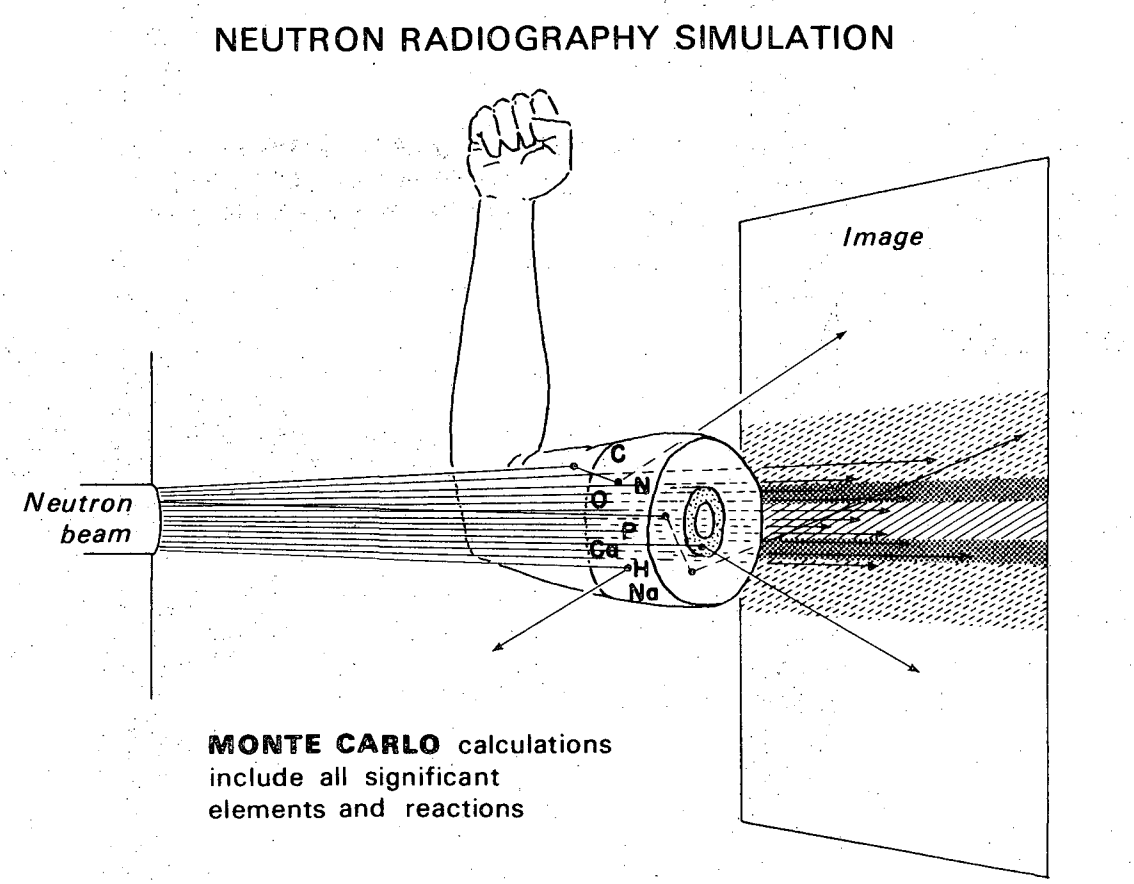

DBL 6910 5123

Fig. 1

NEUTRON EXPOSURE

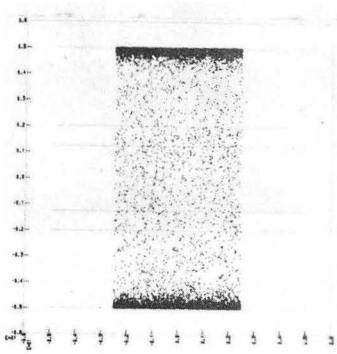

(0.2m - 120 KeV)

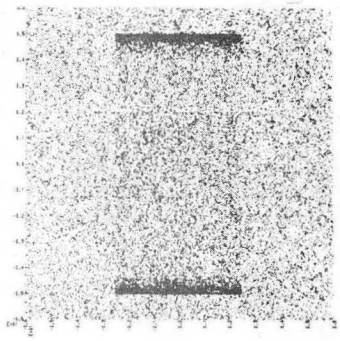

(3m - 120 KeV)

ROUTINE X-RAY

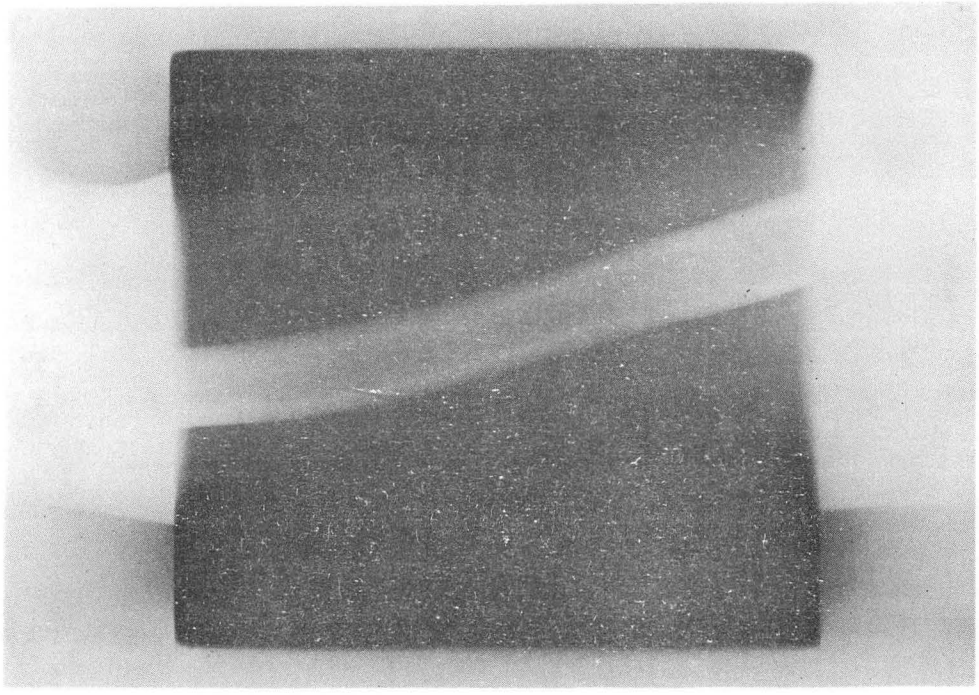

XBB 6911-7078

Fig. 2

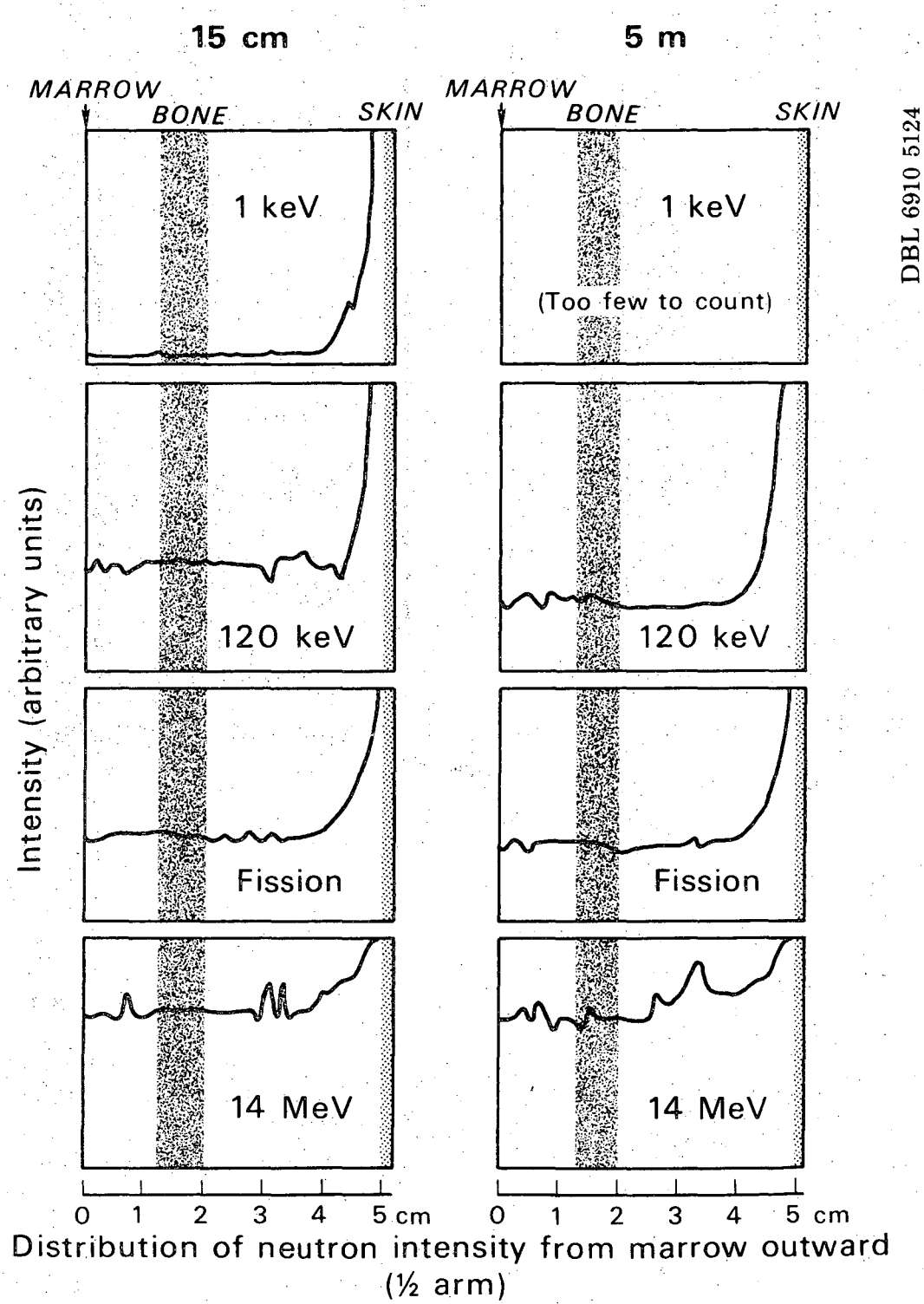

DBL 6910 5124

Fig. 3

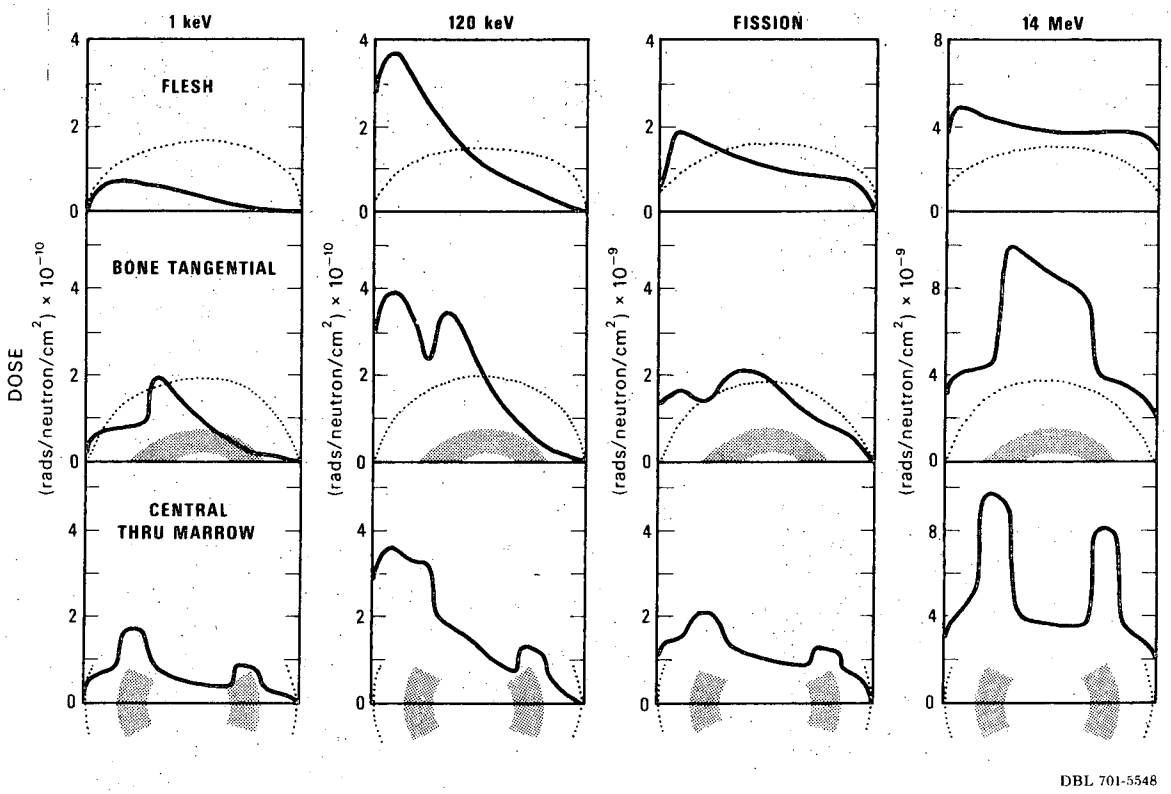
1 keV
120 keV
FISSION
14 MeV
FLESH
BONE TANGENTIAL
CENTRAL
THRU MARROW
DOSE
(rads/neutron/cm^2) × 10^{-10}
(rads/neutron/cm^2) × 10^{-10}
(rads/neutron/cm^2) × 10^{-9}
(rads/neutron/cm^2) × 10^{-9}
DBL 701-5548

Fig. 4

LEGAL NOTICE

This report was prepared as an account of Government sponsored work. Neither the United States, nor the Commission, nor any person acting on behalf of the Commission:

A. Makes any warranty or representation, expressed or implied, with respect to the accuracy, completeness, or usefulness of the information contained in this report, or that the use of any information, apparatus, method, or process disclosed in this report may not infringe privately owned rights; or

B. Assumes any liabilities with respect to the use of, or for damages resulting from the use of any information, apparatus, method, or process disclosed in this report.

As used in the above, "person acting on behalf of the Commission" includes any employee or contractor of the Commission, or employee of such contractor, to the extent that such employee or contractor of the Commission, or employee of such contractor prepares, disseminates, or provides access to, any information pursuant to his employment or contract with the Commission, or his employment with such contractor.

TECHNICAL INFORMATION DIVISION
LAWRENCE RADIATION LABORATORY
UNIVERSITY OF CALIFORNIA
BERKELEY, CALIFORNIA 94720